AD NUMBER

AD320263

CLASSIFICATION CHANGES

TO: unclassified

FROM: confidential

LIMITATION CHANGES

TO:

Approved for public release, distribution unlimited

FROM:

AUTHORITY

NRL ltr dtd 29 Jun 98; NRL, 29 Jun 1998

AD 320 263

CONFIDENTIAL

NRL Report 5540

QUALITY OF RADAR INFORMATION AS INFLUENCED BY AN IONOSPHERIC PROPAGATION PATH

[Unclassified Title]

G. K. Jensen, C. L. Uniacke and E. N. Zettle

Radar Techniques Branch
Radar Division

October 12, 1960

U. S. NAVAL RESEARCH LABORATORY
Washington, D.C.

CONFIDENTIAL

CONTENTS

ABSTRACT
[Confidential]

A study has been made of some of the characteristics of a radar propagation path that includes a reflection in the ionosphere to determine the effects of the ionosphere on range accuracy and the coherence and reliability of the echo. A radar operating frequency of 26.6 Mc was used with a pulse length of 250 μsec, a pulse power of 6 kw, and an antenna gain of 12 db. The very long range of the one-hop F_2 propagation path employed in the experiments, exceeding 1100 naut mi, included a transponder located on the ground to simulate a distant target.

Ground range was calculated from slant range and the virtual height of the ionosphere at the path ends. Calculated ground ranges were within 0.035 percent of known ground range at the best and 2.8 percent at the worst. A spectral analysis of the received signal showed very little spreading of energy. The sideband amplitude 0.2 cps away from the carrier-frequency component was found to be down by 40 db. The amplitude of the signal as received with a horizontally polarized antenna was recorded. On two of the days the signal faded out completely for 16 and 21 percent of the time.

PROBLEM STATUS

This is an interim report on one phase of the problem; work is continuing on this and other phases.

AUTHORIZATION

NRL Problem R02-17
Projects RF 001-02-41-4006
AF MIPR-30-635-8-6136

Manuscript submitted July 8, 1960.

QUALITY OF RADAR INFORMATION AS INFLUENCED BY AN IONOSPHERIC PROPAGATION PATH
[Unclassified Title]

INTRODUCTION

Detection of low-flying targets at very long ranges, exceeding 1000 naut mi, poses an insurmountable problem to the line-of-sight radar. However, if the operating frequency is lowered sufficiently to permit a propagation path which includes a reflection at the ionosphere, then an attractive situation exists in which detection of low-flying targets at very long ranges may indeed be possible. The quality of the echo signals received at the radar site will be determined in part by the ionosphere, particularly by the characteristics and stability of the ionosphere over the midpoint of the propagation path. Hence in determining the feasibility of ionospheric radar, it is necessary to explore the characteristics of the ionosphere that influence the quality of the information expected from the radar.

Ground range to the target may be computed from measured slant range and a knowledge of the virtual height and other parameters of the ionosphere. Shifts in virtual height, which continually occur, will change slant range. Hence regular ionospheric soundings at the midpoint are desirable for the highest accuracy in computation of ground range. However, midpoint soundings are impracticable with the typical radar situation. What is needed is a knowledge of the predictability of the correlation between the soundings which can readily be made at the radar site and the midpoint height soundings. Slant range will also apparently be modified by the ray focusing occurring in the thick, curved ionosphere (1). An idea of the magnitude of these deviations is needed to allow suitable corrections, if needed, to be introduced into the ground-range computation.

The radar receiver visualized for this application has an exceptionally narrow output bandwidth (1/20 cps), because a sophisticated velocity analyzer is used to obtain, among other things, very accurate velocity resolution. This requires that each component of the signal spectrum be confined to a narrow bandwidth to maintain crosscorrelation efficiency. Any uncontrolled modulation of the signal will of course disperse this energy and reduce the system gain. The question which then arises is: what is the amount of dispersal caused by the ionosphere? This has been measured under one set of conditions.

Signal fadeouts do occur from time to time over an ionospheric propagation path. They can be caused by a number of things, such as disturbances in the ionosphere, rotation of the plane of polarization of the wave by the Faraday effect, so that an improperly polarized receiving antenna will intercept little signal energy, etc. Measurements have been made of the fluctuation of the signal amplitude over a period of time.

Successful operation of an ionospheric radar is based upon the premise that energy radiated at an oblique angle will be reflected by the F_2 layer, assuming an appropriate frequency below the maximum usable frequency, and will then impinge upon the earth, where part of the energy will be scattered back along the original path. Received along with the ground-backscattered signal will be signals reflected from moving targets above this ground area and in the incident radar beam. Until a few years ago no agreement existed on the origin of backscatter signals. Many thought they originated directly from the E layer or an F_2 - E mode (2). More recently, others have further explored this question and have concluded that backscatter does originate at the surface of the earth (3). The measurements to be described also definitely varify this conclusion.

A transponder was used, in the experiments to be discussed, to provide a simulated echo. It was located at a sufficient distance from the radar to place it in the F_2 backscatter area.

EQUIPMENT

Figure 1 shows the coherent radar system used in this investigation. The transmitter was capable of an output adjustable up to 6 kw of pulse power with a prf of 500 cps and a pulse width of 250 μsec. The prf was variable in steps down to 15.6 cps. Antenna directivity was obtained by employing a Yagi with 12 decibels of gain and a capability of being rotated through 360 degrees. An operating frequency of 26.6 Mc was used for these measurements.

Two local-oscillator frequencies and the timing pulses are derived from a highly stable master crystal oscillator. The local-oscillator signal for the second converter of the receiver channel is obtained from the storage system, which stores each transmitter-pulse rf output from the monitor receiver. Adequate system stability and coherence for the crosscorrelation process are thus assured. Delay in reading the rf burst signal out of storage after write-in, determined by the timer, is adjusted to coincide with the desired echo or transponder signal, thus effectively gating the receiver on at the appropriate time.

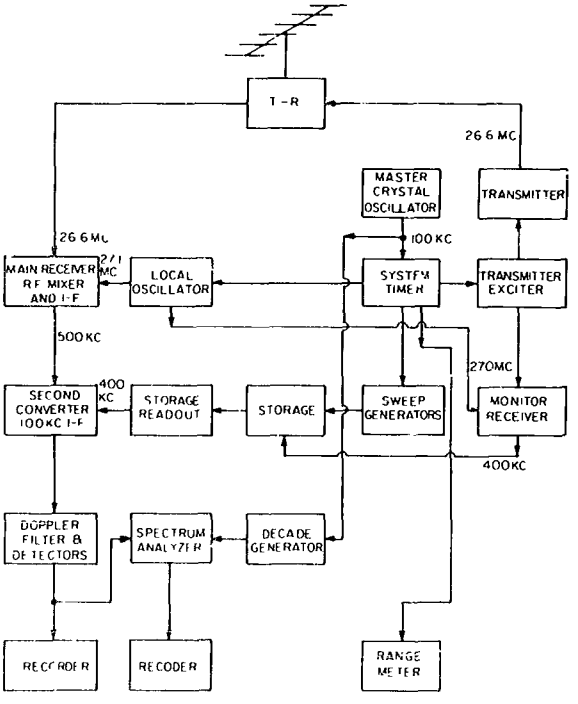

Fig. 1 - Coherent radar system

The spectrum analyzer has an output bandwidth of 1/20 cps and is capable of measuring the amplitudes of any sidebands existing around the intermediate frequency of the receiver. Provision is also made for recording the sideband amplitudes.

Slant range was read on the range meter. It was sufficiently linear and well calibrated to permit a reading accuracy of ± 1.0 naut mi. Frequency of signal fading was monitored by continuously recording the amplitude fluctuations of the received transponder signal in a separate recording channel. A more complete description of this system is given elswhere, along with an earlier backscatter study (4).

The transponder used in these experiments consists of a sensitive receiver tuned to 26.6 Mc which, upon receiving the radar pulses, triggers the companion transmitter. The transmitter pulse width was 250 μsec with a 25-watt pulse power. A quarter-wave vertical antenna was employed.

THEORY

In this particular case, it is of great interest to compute the ground range to the transponder for comparison with the known ground range in order to determine the overall accuracy such an operation can provide. Ground range D may be found from Eqs. (1) and (2):

$$\cos \phi = 1 - \frac{(L/2)^2 - h'^2}{2R(R + h')} \tag{1}$$

$$D = \frac{\phi \pi R}{90} \tag{2}$$

where

L = slant range to transponder

R = radius of the earth

h' = virtual height of the ionosphere

2ϕ = the angle in degrees at the center of the earth subtended by the transmission path,

which have been derived from the geometry of Fig. 2 for the curved-earth, plane-ionosphere case.

The virtual height of reflection of a wave propagated at oblique incidence over a path may be obtained by methods outlined by the National Bureau of Standards (5). The virtual height of reflection at oblique incidence may be related to the virtual-height records made at vertical incidence by making use of the Breit-Tuve theorem and the equivalence theorem. The Breit-Tuve theorem states that the time for transmission along the curved path abcde in Fig. 2 is the same as the time to traverse the triangular path abcde at the velocity of light. The equivalence theorem states that the equivalent height of reflection of a signal of frequency f' incident at an angle ϕ is the same as that of a wave of frequency f at vertical incidence, where

$$f = f' \cos \phi. \tag{3}$$

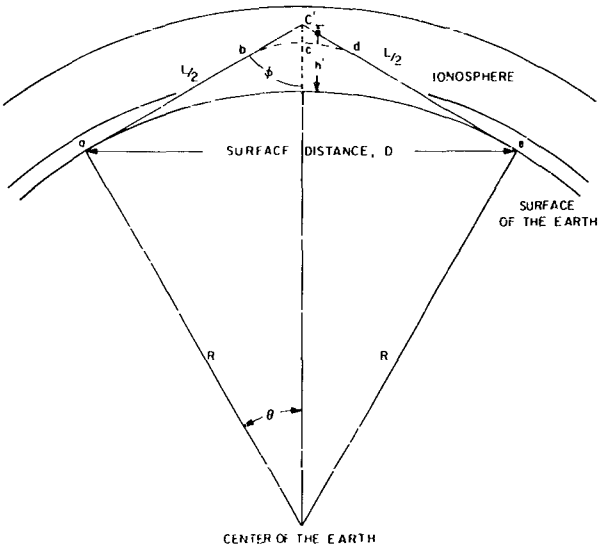

Fig. 2 - Geometry of propagation path

The importance of the equivalence theorem for the case of the flat ionosphere is that a frequency f picked off the vertical incident ionogram at any virtual height h' is the equivalent vertical-incident frequency corresponding to an actual transmitted frequency f' propagated at oblique incidence which enters the ionosphere at such an angle ϕ that the height of the equivalent triangular path is equal to the previously mentioned virtual height h'.

Thus, in order to calculate ground range for a given transmission path and state of the ionosphere, the frequency $f' = f \sec \phi$, and the height h' must satisfy simultaneously the h'f sweep-frequency curve and the geometrical relationship between D, h', and ϕ. A fixed operating frequency f' was used, and h' may be determined as follows. A coordinate scale coinciding with the h'f curve is used to plot a family of curves of h' against f, where f is obtained from Eqs. (3) and (4) for values of sec ϕ corresponding to different values of h' and distance D. Allowing for the earth's curvature,

$$\phi = \tan^{-1} \frac{\sin \theta}{1 + \frac{h'}{R} - \cos \theta} , \qquad (4)$$

where θ is determined from Eq. (2). These graphs, known as transmission curves, are made parametric in distance D, and when in the form of a transparent overlay may be placed over the h'f graph. At the intersections of the curves with the h'f graph, values of h' and f will be found for the fixed operating frequency.

Since the equivalence theorem and Eq. (3) are not strictly true for a curved earth and curved ionosphere, a correction factor K is needed, thus (5):

$$f' = Kf \sec \phi. \quad (5)$$

Transmission curves corrected in the above manner for curved earth and curved ionosphere were used.

Sweep-frequency curves (ionograms) were available for locations at Fort Belvoir, Va., and White Sands, N.M., which closely approximated the ends of the transmission path, but none were available near the midpoint. Originally it was desired that the accuracy of the computed ground range be compared using heights scaled from midpoint ionograms as contrasted with heights from the ionograms at the path ends. The last condition simulate the limitation which would exist at many radar sites where midpoint ionograms would be impossible to obtain. In lieu of the midpoint ionogram, the times of both the Fort Belvoir and White Sands ionograms were adjusted to the midpoint times to simulate midpoint ionograms. The results using these ionograms were then compared with those of the unadjusted end-point ionograms. Since the ionosphere is constantly changing, this is not an ideal solution to the problem, as will be seen, but it does show what can be done to compensate for a lack of midpoint ionograms.

Normally the skip distance and the extent of distance behind the skip over which it is possible to establish transmission paths may be determined by the set of transmission curves parametric in range and the appropriate ionogram. Also, the unique virtual height for each path distance may be found by noting the intersection of the transmission curve of this distance with the h'f curve and reading h' on the ionogram. It will be noted (Fig. 3) that the height at the skip distance (point a) is greater than the heights for greater ranges, (points b and c). Ranges given on the transmission curves are ground range.

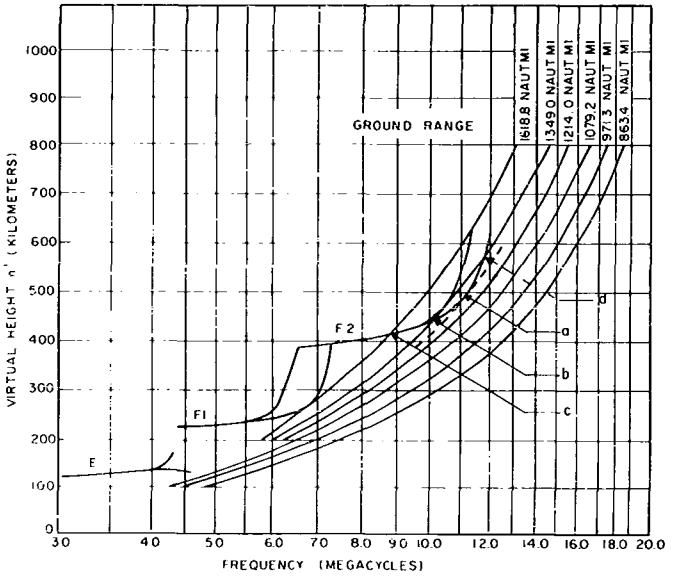

Fig. 3 - Transmission-curve overlay on ionogram

The problem in the case of radar is one of not knowing the ground range to the target (or transponder in this experiment, since ground range is to be computed to simulate the actual situation and then compared with the known ground range) and thus not knowing how to read the correct height from the ionogram. Slant range is known from the radar, but to convert this to ground range so that h' may be found from the ionogram requires knowledge of the very parameter sought.

A solution to the dilemma is possible if the skip distance can be identified and if then the distance behind the skip to the actual transmission path (transponder signal) is also found. The skip distance can be read from the transmission curves and ionogram. The distance D_s behind the skip can be obtained from a second piece of radar information, the slant range to the skip, which is readily determined. Subtracting the slant range to the skip from the slant range to the transponder yields the distance the transponder is located beyond the skip in terms of a slant range. This difference in range was desired in terms of ground range; however, at the low radiation angles utilized in this equipment, the error in using the difference in slant ranges directly is slight. Also, it is evident (Fig. 3) that for differences that place the point at which h' is read in the region of b and c, the height is very insensitive to distance. For differences that place the reading between a and b, h' is more sensitive to distance, but the absolute magnitude of the difference is then very small.

Ground range to the skip can be had by taking the difference between the slant skip range and the slant transponder range and subtracting it from the known ground range to the transponder. This was done for data taken on Dec. 23 and 26, 1957, with the transponder located at Clarendon, Texas, as shown in Figs. 4, 5, 6, and 7.*

The figures also show the skip distance as read from the ionograms of the same days for both the ordinary and extraordinary rays at both ends of the path. Agreement between measured and ionogram skip distance is not good, probably due in large part to the fact that the ionograms are not from the midpoint of the transmission path. Therefore, in order to determine h', these differences are reconciled by obtaining the difference distance D_s from the measured slant skip distance which is an accurate reflection of midpoint ionospheric conditions and adding it to the skip range read from the ionogram. Since D_s is determined from measurements reflecting midpoint conditions, it will, when added to the ionogram skip distance, locate the point on the h'f curve from which to read h' with good accuracy, under the circumstances, even though the ionogram skip distance does not agree well with the radar skip.

Ray focusing can influence the accuracy with which skip-range and possibly beacon-range measurements can be made, under certain circumstances, as discussed by Peterson (1). When the ratio between the operating frequency (f_{op}) and the F-layer critical frequency (f_c) is small, the slant range to the leading edge of the backscatter echo which corresponds to the minimum-time-delay ray is appreciably less than the slant range to the true skip. Conversely, the ground distance corresponding to the minimum-time-delay ray is greater than the ground skip distance. This would indicate that as the backscatter moves in over a fixed ground beacon, or as an aircraft flies through the leading edge of the backscatter, the slant range at which it first appeared would be greater than the minimum-time-delay distance shortly thereafter. At a still later time, the slant range should again increase. This would of course introduce and undesired anomaly into the determination of ground range.

*Figures 4-53 are bound consecutively at the end of this report.

The error in determining ground skip distance is about 3 percent if the minimum-time-delay ray is used instead of the skip-delay ray, and if the ratio of $f_{op}/f_c = 1.4$ for a skip distance of 880 km, according to Peterson.

Figure 8 shows a typical F_2 one-hop backscatter echo in which $f_{op} = 26.6$ Mc. The problem is of course the fact that only the distance corresponding to the minimum time delay can be measured. However, the error in determining the skip distance diminishes with larger ratios of f_{op}/f_c such as prevailed in the experiments to be discussed.

RESULTS

Range Measurements

Slant-range measurements were made with a transponder simulating a target in the region of the first-hop F mode of propagation. The transmitter was located in Washington, D.C., and the transponder was placed for a period of time in Clarendon, Texas, and then in Albuquerque, New Mexico. Figure 9 shows the slant range to the transponder as a function of time, when it was located in Clarendon, Texas. The ground range to this site was 1168 naut mi and the true bearing 265 degrees. The skip distance to the leading edge of the backscatter remained constant at 971 naut mi on this day (Dec. 23, 1957) from 1000 to 1200 EST. During this time the transponder signal as received in Washington, D.C. was near the center of the back-scatter echo. Beginning at 1208, the skip distance began moving out and soon exceeded the range of the transponder, at which time the transponder signal then disappeared.

The manner in which the slant range is as dependent upon the virtual height of the F layer as the skip distance is of special interest. Hence when a change in skip distance occurs, a corresponding change in slant range should be found. Figure 9 shows that there is no definite trend in slant range until the skip begins to move out; then the slant range increases steadily until the skip range exceeds the transponder slant range. Also, it will be noted that the transponder slant range exceeded the true ground range to the beacon by about 60 naut mi between 1000 and 1200, and at the time the signal was lost at 1440 it exceeded the true range by about 110 naut mi. Another phenomenon of interest is the fact that the transponder signal failed when the slant skip ranges exceeded the slant transponder range. This strongly supports the thesis that backscatter signals are due to impingement of the rays on the earth rather than on the E layer or other combinations of layers.

Ground range to the transponder was calculated by the method previously described. As nearly as possible, the proper virtual height was determined for each ray path from ionograms obtained at Ft. Belvoir and White Sands. The ionogram time at which each h' was read corresponded with the time of the slant-range measurements for which computation of ground range was made. Since ionograms were available for both ends of the path, two separate sets of calculations were made to allow comparison between the two. Midpoint ionograms were not available. Therefore, to simulate these ionograms the times of both the Ft. Belvoir and the White Sands ionograms were adjusted, and again two separate sets of ground-range calculations were made to determine whether adjustment of ionogram time to simulate midpoint conditions was beneficial and to determine whether the location at which the ionograms were taken influenced the results.

Almost always, F-layer h'f curves show evidence of a forking, the outer curve being due to the extraordinary ray and the inner one being due to the ordinary ray. Often the transmission curve of the desired distance passes through the forked region, raising the question as to whether the ray took the ordinary or extraordinary path. In some cases both paths may be effective, resulting in multiple received pulses which have been observed.

Also, multiple paths can result from the upper and lower rays of each branch, as represented by points b and d on Fig. 3. Calculation of ground range for each of the four cases previously mentioned was repeated for both the ordinary ray and the extraordinary ray.

Figure 10 shows the error, or deviation, of the calculated ground range from the known ground range with the transponder located in Clarendon, Texas, on Dec. 23, 1957 for adjusted ionogram time (Ft. Belvoir ionogram). Using the extraordinary ray, the maximum deviation is 6 naut mi throughout the day, with an average near zero. The maximum error using the ordinary ray is 10 naut mi, with an average much less. With the same conditions, but using the White Sands ionogram, Fig. 11 shows the maximum error with the ordinary ray 21.5 naut mi and with the extraordinary ray 26 naut mi.

When unadjusted time is used, Fig. 12 indicates that with the Ft. Belvoir ionograms the maximum ordinary ray error is 12 and the extraordinary ray 10 naut mi. The maximum error when using the unadjusted White Sands ionogram (Fig. 13) is 34.5 naut mi for the extraordinary ray and 31.5 naut mi for the ordinary ray.

The results of this one day suggest that adjusting ionogram time improves the accuracy of the calculated range. Of the two sets of ionograms, the Ft. Belvoir set provided the most accurate ranges. This may be explained in part by the fact that the White Sands ionograms were noticed to change more rapidly with time and to change more drastically in general configuration than the Ft. Belvoir curves. Also, the quality of the WS ionograms was inferior, probably causing loss in the accuracy of the h' readings.

Slant-range measurements were made between 0920 and 1150 on Dec. 24, 1957, as indicated in Fig. 14. The difference between slant range and ground range averaged about 70 naut mi. Computed range deviations for the four sets of ionograms are shown by Figs. 15, 16, 17, and 18. Here the ionograms adjusted for time produce mixed results, while the Ft. Belvoir ionograms again result in the least deviation.

Measurements made on Dec. 26, 1957 between 0920 and 1300 are shown in Fig. 19. The skip distance began 200 naut mi ahead of the signal and at 1100 commenced moving out, until at 1300 the signal disappeared. During this time the difference between slant range and ground range to the transponder changed from about 70 to 140 naut mi. It will be noted that here also, when the skip range exceeded the beacon range, the beacon signal disappeared, indicating that the backscatter must be from the ground reflection. Ground range was computed for the four sets of conditions, and the results are shown on Figs. 20, 21, 22, and 23. Here, as on Dec. 23, ionograms adjusted for time produce the least error in calculated ground range. Likewise, ionograms taken at Ft. Belvoir result in the least error.

An interesting phenomenon is illustrated in Fig. 21. The dotted portions of the curves were calculated from h', read from the F_1 portion of the White Sands ionograms. These particular ionograms show a distinct separation of the F curve into F_1 and F_2 regions at the ranges of interest, so there was a question of which layer was responsible for the propagation path. The graph clearly shows that the path penetrated to the F_2 layer, because the error is least using the F_2 layer h'.

On Dec. 27, 1957, measurements were made between 0930 and 1240. Slant range to the transponder is plotted in Fig. 24. Skip range began at 200 naut mi. ahead of the signal and moved in until it was 300 naut mi ahead at 1240. Again, range was computed for the four sets of ionograms and is shown in Figs. 25, 26, 27, and 28. Reference to these figures indicates that the center of these curves seems to be displaced 10 to 20 naut mi, depending on the curve. Otherwise, the maximum plus and minus deviation of the curve is comparable to that of the earlier curves. Beyond this, the results were inconclusive.

The transponder was next moved to Albuquerque, New Mexico, which is 1433 naut mi from the radar site at Washington, D.C. Data were taken from 0925 to 1620 on Dec. 30, 1957. Figure 29 shows the slant range to the transponder as a function of time of day, and it will be noted that slant range exceeds the transponder ground range from 53 to 89 naut mi, depending on time. The Skip distance remained a constant 300 naut mi ahead of the transponder signal during the entire period. Ground range was calculated again, using the four different sets of ionograms. The least error was found using the Ft. Belvoir ionogram, adjusted in time as Figs. 30, 31, 32, and 33 illustrate.

Measurements were also made on Dec. 31, 1957 between 0940 and 1215. Slant range to the transponder is plotted in Fig. 34, and again the skip range remained a constant 300 naut mi ahead of the transponder signal. Figures 35, 36, 37, and 38 show the error in the calculated ranges. Again, the calculation using the Ft. Belvoir ionogram adjusted in time resulted in the least error.

A reexamination of the error in calculation of ground range indicates that this error can be as little as a fraction of a mile to more than 40 miles. The results are best using the Ft. Belvoir ionograms and are further improved on an average by adjusting time to simulate a midpath ionogram. On some days the errors are much less than on others, which suggests that the ionosphere is at times comparatively quiescent over large areas. Conversely, it is also obviously turbulent at other times, which points up the desirability of midpath ionograms. The curves show examples of the range accuracies that can be realized without midpath ionograms.

Ray Focusing

Ray focusing effects can be studied on days when the skip distance moves in one direction or the other over the transponder site. On Dec. 23 and 26, the skip distance did move out beyond the transponder location. A study of Figs. 9 and 19 shows that on these days the slant range steadily increased as the skip range moved out. There was no reversal in the variation of slant range with skip distance. Any such phenomenon, if it were present, would introduce an ambiguity in the determination of range near the skip distance. The ratio of operating frequency to F_2 critical frequency on these two days was about 1.8, which is high enough to minimize the effects of ray focusing. The effects are reportedly most pronounced with ratios closely approaching 1.0.

Fading

The radar transmitting and receiving antenna was horizontally polarized. Amplitude variations of the received transponder signal were recorded to permit a study to be made of the extent and character of the fading to be found on this type of transmission path. An amplitude-time analysis made of the signals received on four separate days is plotted in Figs. 39, 40, 41, 42, and 43. An arbitrary level was selected as the 100-percent value; however, a few points were later found to exceed this level, thus accounting for the extra bar on the graphs. These figures show that the signal actually fades completely at times. This was particularly true on Dec. 26 and 30, when the signal was out 16 and 21 percent of the time respectively. Such a situation is not desirable in a radar. One cause of this type of fading, of course, is rotation of the plane of polarization of the signal in the ionosphere, which causes an antenna polarized in one direction only to fail to intercept all of the incident energy. A suitably polarized receiving antenna should maximize the percentage of time a signal is detectable. Receiver gating was used to select only one of the several ray components visible at times for recording; this minimized to some extent destructive fading entering into the data. Also, the data reflects only one-way path conditions.

Spectrum Analysis

Two separate samples of the transponder signal received on Dec. 23, 1957 were run through the spectrum-analyzer portion of the radar system. The amplitudes of the received signal and selected side frequencies (at the i-f frequency) were measured, and Figs. 44 and 45 show the results. The side frequencies are plotted in cycles per second displacement from the i-f frequency. The output noise level in the 1/20-cps bandwidth of the analyzer was about 58 db below the carrier level, which is the zero reference level. The two figures indicate that the sideband energy is already down to -40 db at ±0.2 cps and drops down essentially to the noise level beyond 2.3 cps on Fig. 44 and beyond 1.0 cps on Fig. 45. This result indicates very little spreading of the signal energy due to the ionosphere or any other cause; however, it must be emphasized that these are only two samples of data taken on a single day. Thus it is not conclusive. Also, these data are representative of only a one-way path. It is well known that the ionosphere continually changes from hour to hour, day to day, month to month, and year to year. For this reason, studies such as discussed here should be repeated with changing ionospheric conditions to provide as complete a picture as possible. These studies have been continued and expanded.

Alternate Range Determination

Where an approximate ground-range determination is satisfactory, and when speed and simplicity of operation are desired, without the use of ionograms, the following method is of interest. It will be noted that the difference between slant range and known ground range in Figs. 9 and 19 varies between an average of about 60 naut mi when the transponder signal is 200 miles behind the skip range at midmorning to about 120 naut mi at the skip range in the afternoon. If a curve of the difference vs distance behind the skip were prepared for the complete time the signal was within the backscatter, averaged over a sufficient number of days, then knowing the position of the signal behind the skip from the radar, it would be possible to read a difference range. This difference when subtracted from the measured slant range would be the approximate ground range to the target. Greatest accuracy will be obtained when the ionosphere is "normal," and the method will be least accurate on days of disturbed ionosphere. The curve will require modification for change of operating frequency, season of year, and year in the sun spot cycle.

In connection with range determination, it is interesting to investigate how virtual height varies as a function of skip range and time. Data were taken from the same ionograms used to calculate ground range. Points were read using a 26.6-Mc transmission curve parametric in distance. Virtual height was read at the skip range. Figures 46 and 47 are a plot of virtual height h′ vs time and skip range respectively for the Ft. Belvoir ionograms of Dec. 23, 1957.

From Fig. 46, it is obvious that the virtual height is not a smooth function of time. The same points shown in Fig. 46 are replotted in Fig. 47 vs skip range. Here also, h′ is far from being a linear function of skip range. If it had been, this might possibly have been the basis for another method of calculating the ground range to target without the need for ionograms. Figures 48 and 49 show the same curves using White Sands ionograms for Dec. 23, and Figs. 50 through 53 show the plots for Dec. 26, 1957. Again, the same characteristics are evident.

SUMMARY

Ground range from the radar to the transponder was calculated from a knowledge of the radar slant range and the virtual height of the F layer, obtained from vertical incident

soundings made near the ends of the propagation path. Accuracy of the ground-range calculation was at best within 0.035 percent and at worst within 2.8 percent of the known ground range. In general, the results are improved if the virtual height read off a path-end ionogram is taken at a time that simulates the ionospheric conditions existing at the path midpoint at the moment of the slant-range measurement. Calculated range errors are much less on some days than others, which indicates that the ionosphere is at times comparatively quiescent over large areas and at times obviously turbulent. This suggests that virtual heights determined from midpath ionograms instead of path-end ionograms would increase the accuracy of the range calculations. Alternate methods of determining ground range are also suggested and explored.

The data were studied for evidence of ray-focusing effects. None were found, probably because the ratio of operating frequency to the F_2 layer critical frequency averaged about 1.8 instead of near 1.0, where the effect is supposedly the most pronounced.

Investigation of the data reveals that when the backscatter skip range exceeds the transponder range, the transponder signal disappeared. This leads to the conclusion that the backscatter signal is due to the rays refracted at the F layer impinging upon the earth and scattering a fraction of their energy back along the incident path. This finding confirms what investigators in this field have come to believe only in recent years. Before this, backscatter signals were thought to come from energy being scattered from ionospheric layers instead of from the earth.

The amplitude of the transponder signal was recorded for selected periods of time to determine what percentage of the time the signal faded out completely. On two of the days the signal faded out completely for 16 and 21 percent of the time, respectively. One cause of such fading is changing polarization; this can be minimized with a suitably polarized receiving antenna. The possibility of destructive fading due to the addition of two or more out-of-phase signal components was reduced by using the receiver gating to select only one of the several ray components, present at times, for recording.

A spectral analysis of the transponder signal received at the radar was made to determine how much, if at all, the signal energy was spread out due to perturbations of the ionospheric path.. At ± 0.2 cps from a spectral line, the sideband energy was down 40 db from the amplitude of the line frequency. Beyond 2.3 cps the sideband energy was down 53 db to the noise level of the 1/20-cps bandwidth of the analyzer. Thus very little spreading of energy occurred; however, these data are representative of only a one-way path, for a sample period of less than one day.

ACKNOWLEDGMENTS

The authors wish to acknowledge the work of Mr. G. A. Morgan, who designed the receiver and local oscillators, Mrs C. B. Tesauro, who designed the timer, Mr. F. E. Boyd and Mr. R. G. Cumings, who designed the transmitter, and Mr. W. C. Headrick, who designed and operated the transponder.

REFERENCES

1. Peterson, A. M., "The Mechanism of F-Layer Propagated Back-Scatter Echoes," J. Geophys. Research 56:221-237 (1951)

2. Eckersley, T. L., "Analysis of the Effect of Scattering in Radio Transmission," J. IEE (London), 86:548-567 (1940)

3. Abel, W. G., and Edwards, L. C., "The Source of Long-Distance Backscatter," Proc. IRE, 39:1538-1541 (1951)

4. Jensen, G. K., and Uniacke, C. L., "Spectral Bandwidth of Backscatter Signals," NRL Report 4976, Aug. 1957

5. National Bureau of Standards Circular 462, "Ionospheric Radio Propagation," June 1948

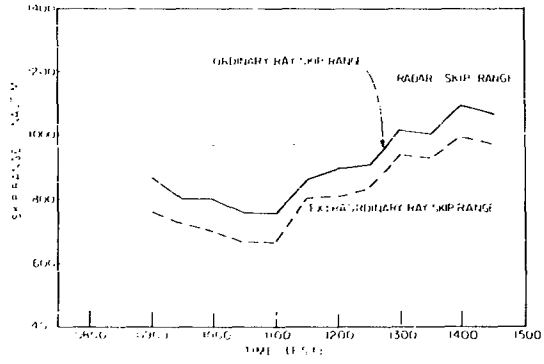

Fig. 4 - Skip range vs time for Ft. Belvoir ionogram, Dec. 23, 1957, transponder at Clarendon, Texas

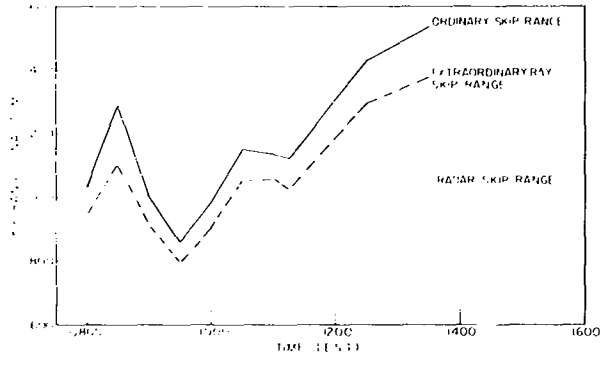

Fig. 5 - Skip range vs time for White Sands ionogram, Dec. 23, 1957, transponder at Clarendon, Texas

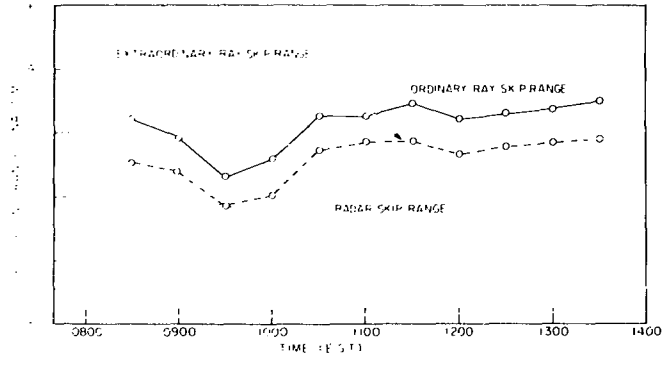

Fig. 6 - Skip range vs time for Ft. Belvoir ionogram, Dec. 26, 1957, transponder at Clarendon, Texas

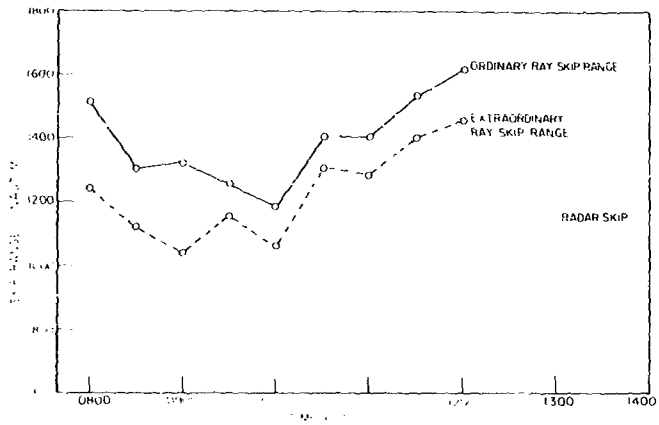

Fig. 7 - Skip range vs time for White Sands ionogram, Dec. 26, 1957, transponder at Clarendon, Texas

Fig. 8 - Typical backscatter

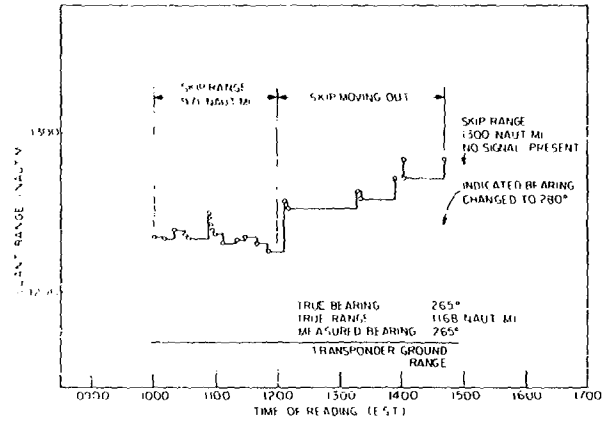

Fig. 9 - Slant range vs time on Dec. 23, 1957, transponder at Clarendon, Texas

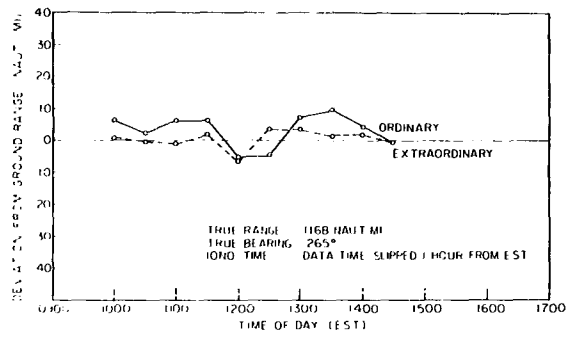

Fig. 10 - Calculated range error vs time, Ft. Belvoir ionogram - adjusted time for Dec. 23, 1957, transponder at Clarendon, Texas

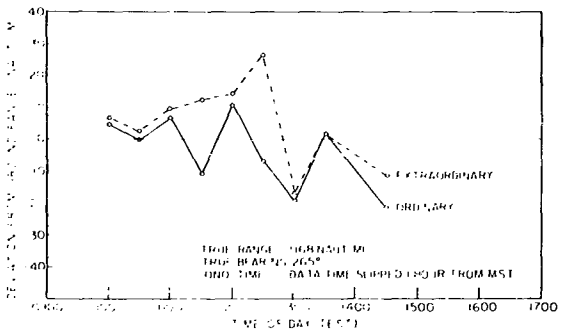

Fig. 11 - Calculated range error vs time, White Sands ionogram - adjusted time for Dec. 23, 1957, transponder at Clarendon, Texas

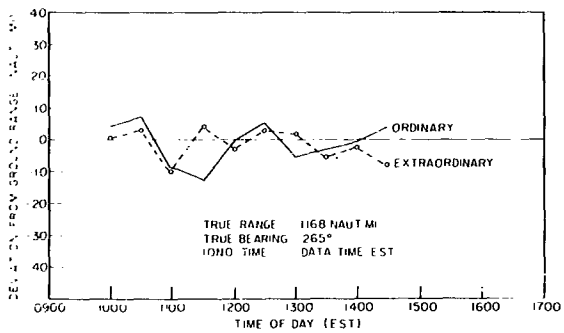

Fig. 12 - Calculated range error vs time, Ft. Belvoir ionogram for Dec. 23, 1957, transponder at Clarendon, Texas

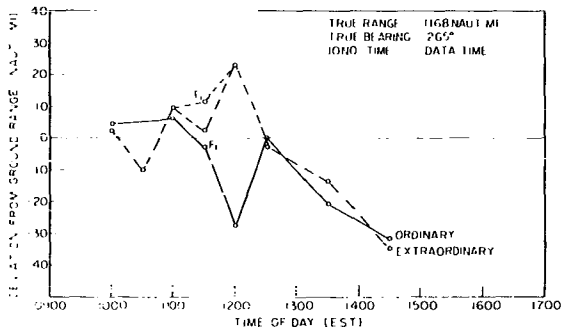

Fig. 13 - Calculated range error vs time, White Sands ionogram for Dec. 23, 1957, transponder at Clarendon, Texas

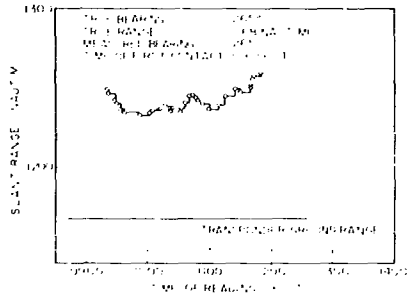

Fig. 14 - Slant range vs time on Dec. 24, 1957, transponder at Clarendon, Texas

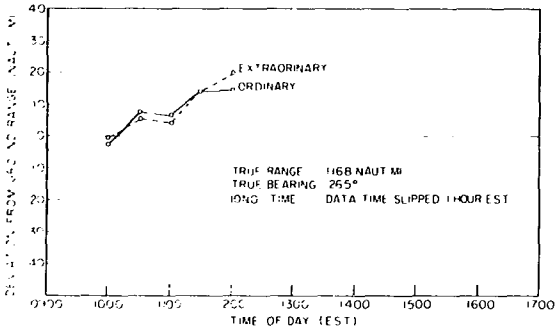

Fig. 15 - Calculated range error vs time, Ft. Belvoir ionogram - adjusted time for Dec. 24, 1957, transponder at Clarendon, Texas

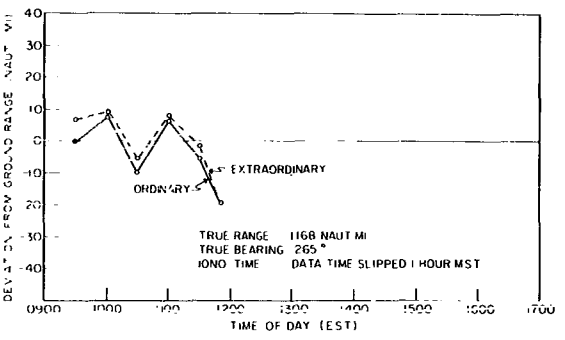

Fig. 16 - Calculated range error vs time, White Sands ionogram - adjusted time for Dec. 24, 1957, transponder at Clarendon, Texas

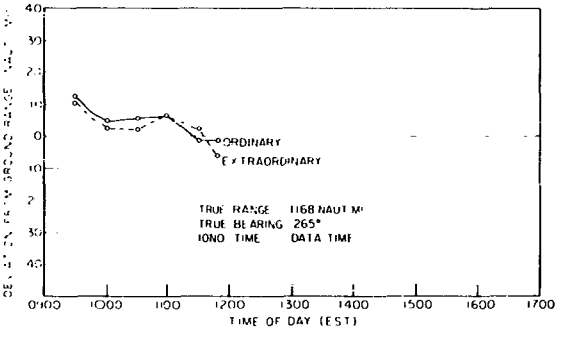

Fig. 17 - Calculated range error vs time, Ft. Belvoir ionogram for Dec. 24, 1957, transponder at Clarendon, Texas

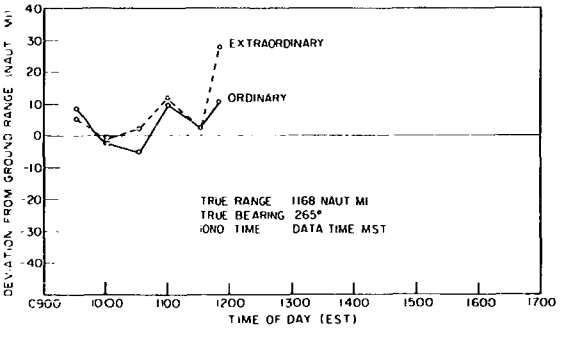

Fig. 18 - Calculated range error vs time, White Sands ionogram for Dec. 24, 1957, transponder at Clarendon, Texas

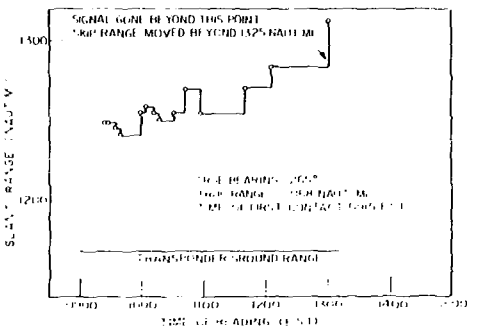

Fig. 19 - Slant range vs time on Dec. 26, 1957, transponder at Clarendon, Texas

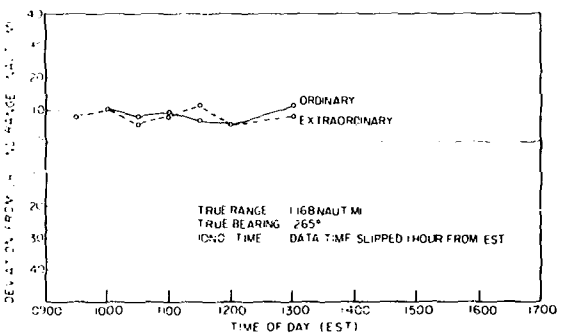

Fig. 20 - Calculated range error vs time, Ft. Belvoir ionogram - adjusted time for Dec. 26, 1957, transponder at Clarendon, Texas

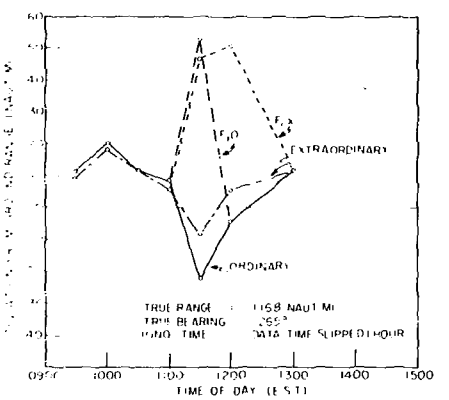

Fig. 21 - Calculated range error vs time, White Sands ionogram - adjusted time for Dec. 26, 1957, transponder at Clarendon, Texas

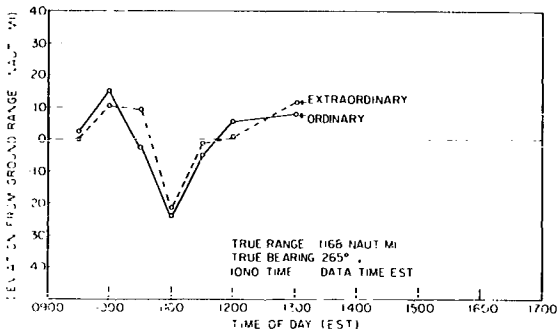

Fig. 22 - Calculated range error vs time, Ft. Belvoir ionogram for Dec. 26, 1957, transponder at Clarendon, Texas

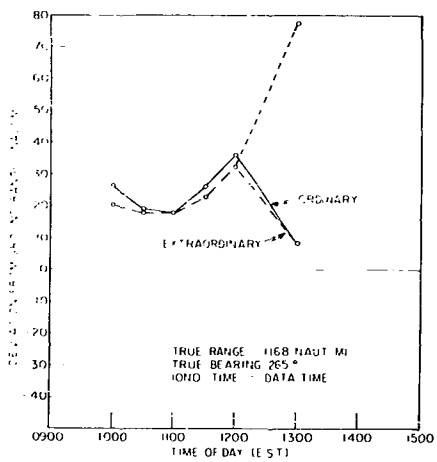

Fig. 23 - Calculated range error vs time, White Sands ionogram for Dec. 26, 1957, transponder at Clarendon, Texas

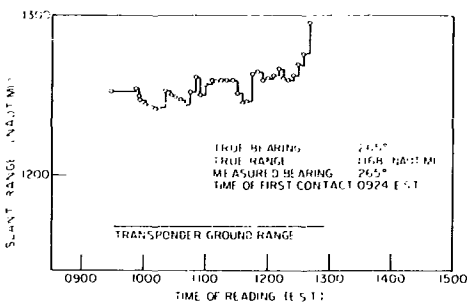

Fig. 24 - Slant range vs time on Dec. 27, 1957, transponder at Clarendon, Texas

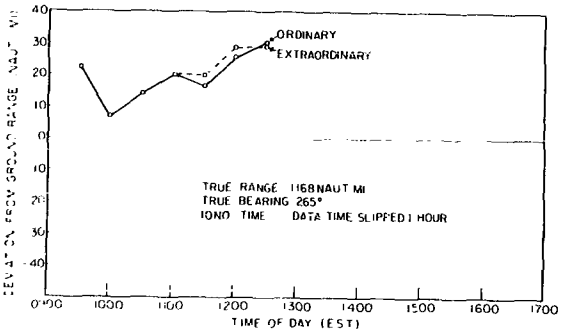

Fig. 25 - Calculated range error vs time, Ft. Belvoir ionogram - adjusted time for Dec. 27, 1957, transponder at Clarendon, Texas

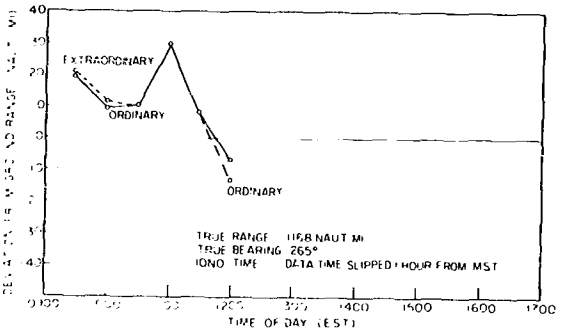

Fig. 26 - Calculated range error vs time, White Sands ionogram - adjusted time for Dec. 27, 1957, transponder at Clarendon, Texas

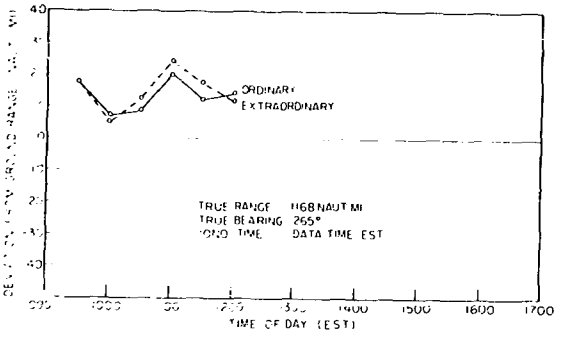

Fig. 27 - Calculated range error vs time, Ft. Belvoir ionogram for Dec. 27, 1957, transponder at Clarendon, Texas

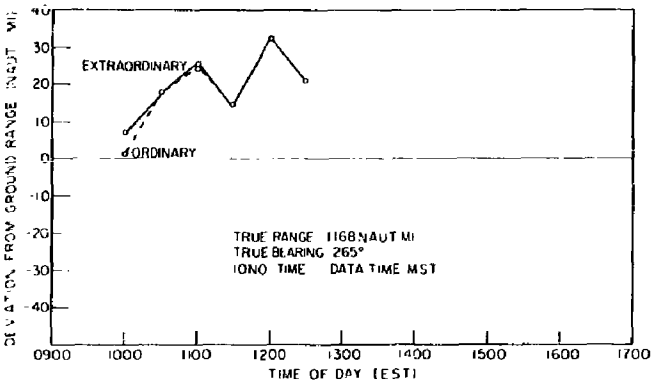

Fig. 28 - Calculated range error vs time, White Sands ionogram for Dec. 27, 1957, transponder at Clarendon, Texas

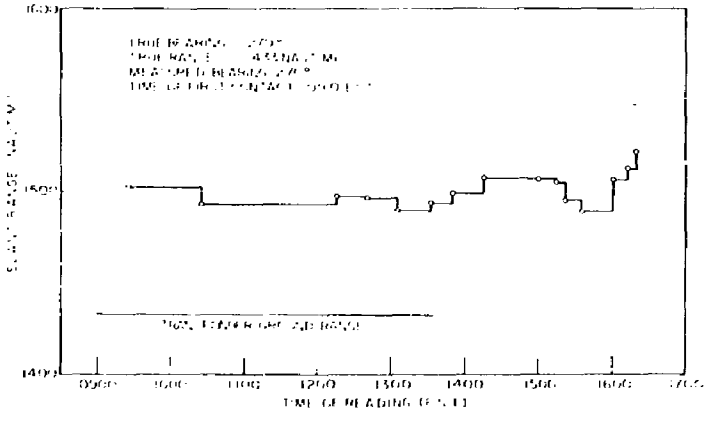

Fig. 29 - Slant range vs time on Dec. 30, 1957, transponder at Albuquerque, New Mexico

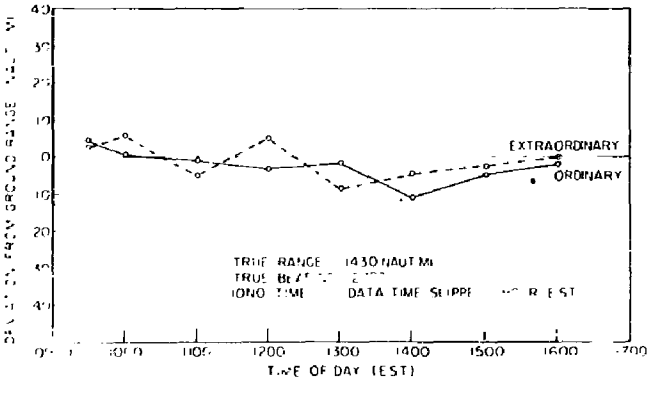

Fig. 30 - Calculated range error vs time, Ft. Belvoir ionogram - adjusted time for Dec. 30, 1957, transponder at Albuquerque, New Mexico

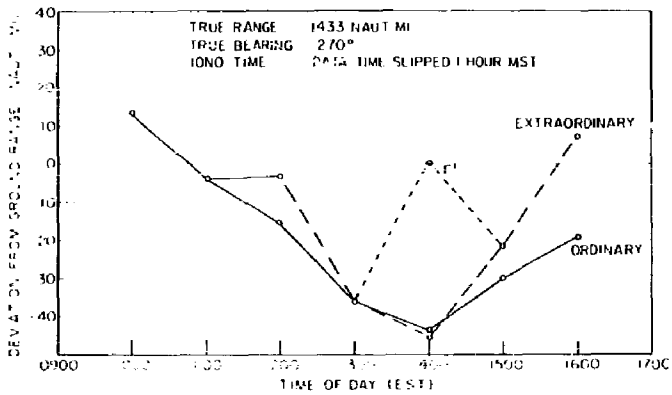

Fig. 31 - Calculated range error vs time, White Sands ionogram - adjusted time for Dec. 30, 1957, transponder at Albuquerque, New Mexico

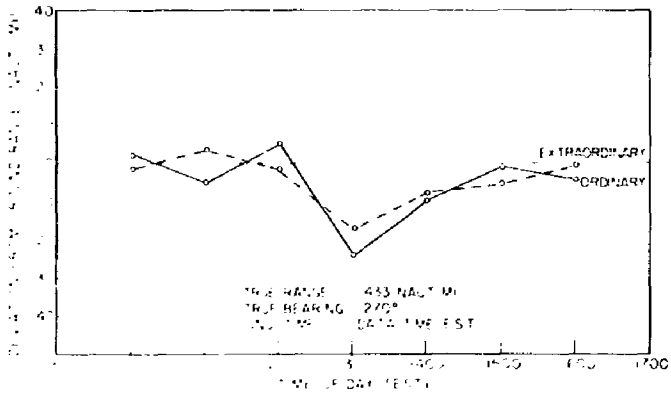

Fig. 32 - Calculated range error vs time, Ft. Belvoir ionogram for Dec. 30, 1957, transponder at Albuquerque, New Mexico

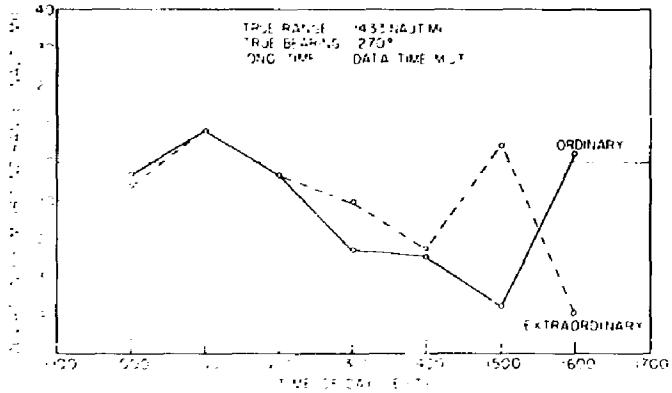

Fig. 33 - Calculated range error vs time, White Sands ionogram for Dec. 30, 1957, transponder at Albuquerque, New Mexico

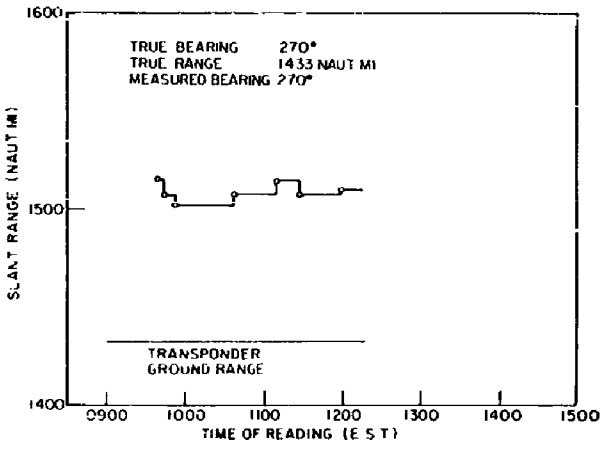

Fig. 34 - Slant range vs time on Dec. 31, 1957, transponder at Albuquerque, New Mexico

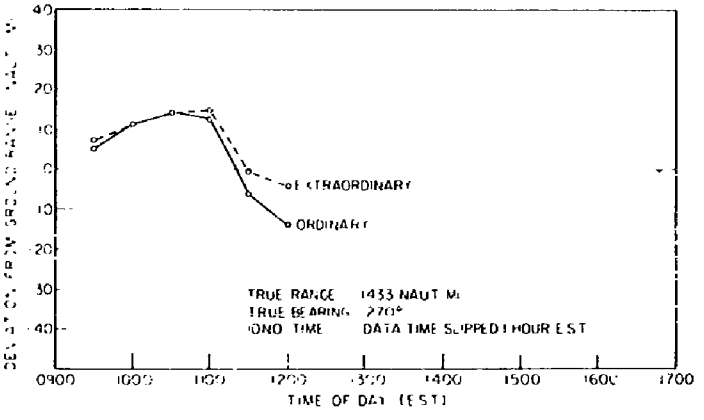

Fig. 35 - Calculated range error vs time, Ft. Belvoir ionogram - adjusted time for Dec. 31, 1957, transponder at Albuquerque, New Mexico

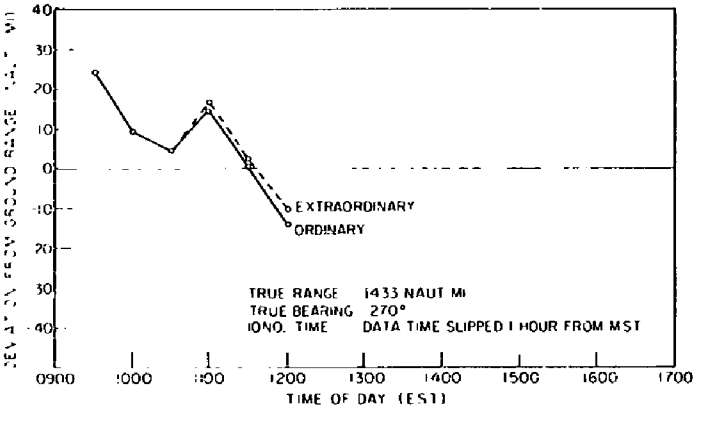

Fig. 36 - Calcualted range error vs time, White Sands ionogram - adjusted time for Dec. 31, 1957, transponder at Albuquerque, New Mexico

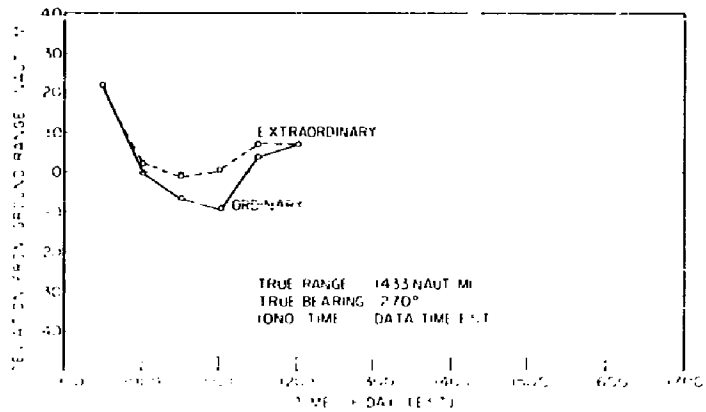

Fig. 37 - Calculated range error vs time, Ft. Belvoir ionogram for Dec. 31, 1957, transponder at Albuquerque, New Mexico

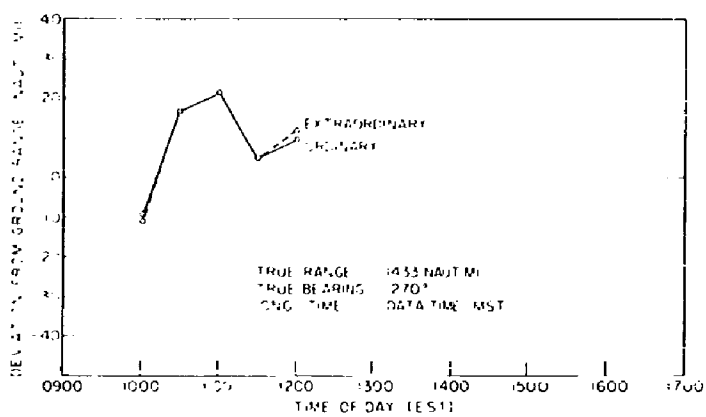

Fig. 38 - Calculated range error vs time, White Sands ionogram for Dec. 31, 1957, transponder at Albuquerque, New Mexico

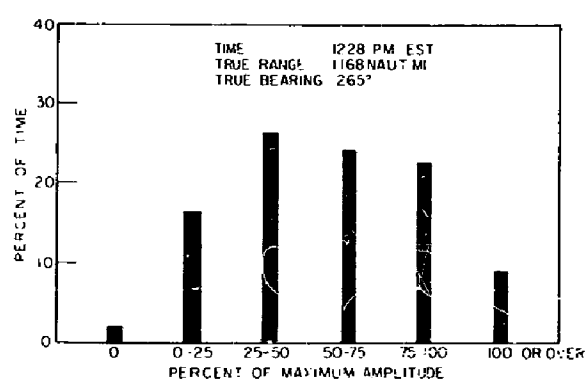

Fig. 39 - Amplitude vs time analysis of signal No. 1 for Dec. 23, 1957, transponder at Clarendon, Texas

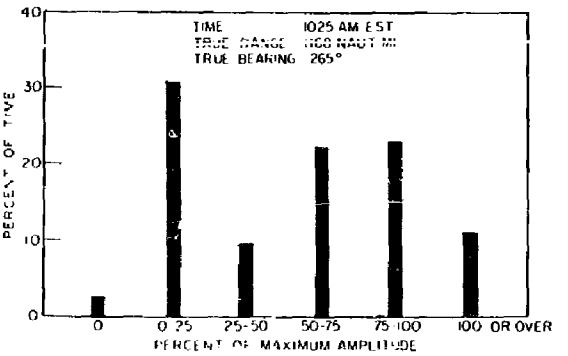

Fig. 40 - Amplitude vs time analysis of signal No. 2 for Dec. 23, 1957, transponder at Clarendon, Texas

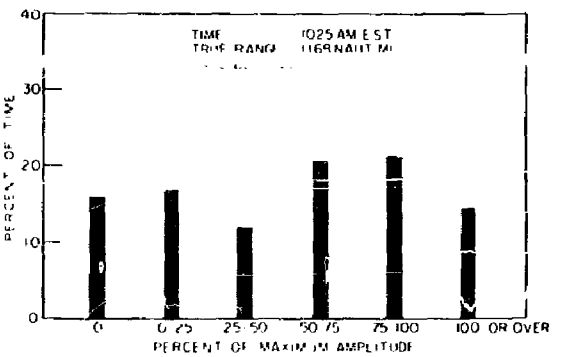

Fig. 41 - Amplitude vs time analysis of signal for Dec. 26, 1957, transponder at Clarendon, Texas

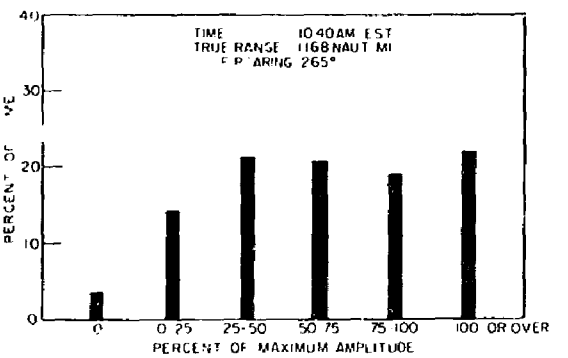

Fig. 42 - Amplitude vs time analysis of signal for Dec. 27, 1957, transponder at Clarendon, Texas

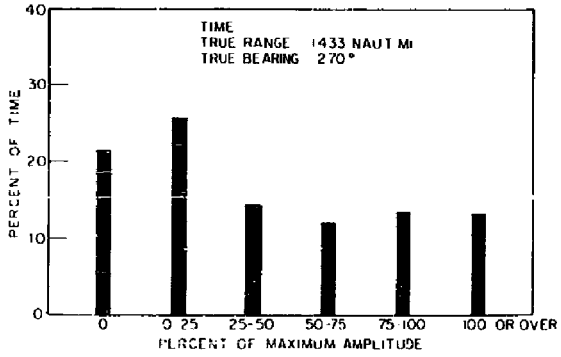

Fig. 43 - Amplitude vs time analysis of signal for Dec. 30, 1957, transponder at Albuquerque, New Mexico

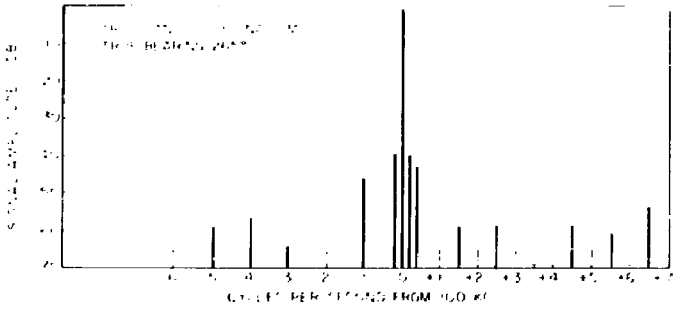

Fig. 44 - Spectrum analysis of received transponder signal, Run 1, for Dec. 23, 1957, transponder at Clarendon, Texas

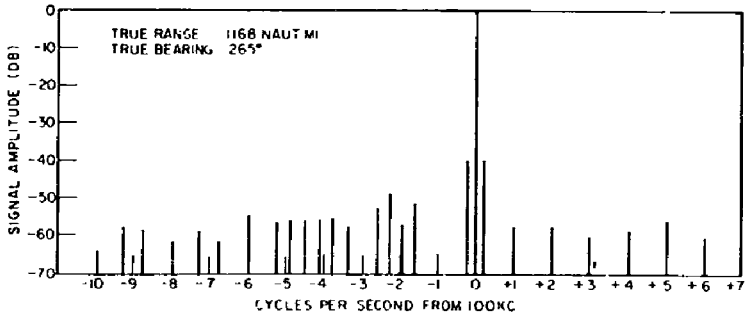

Fig. 45 - Spectrum analysis of received transponder signal, Run 2, for Dec. 23, 1957, transponder at Clarendon, Texas

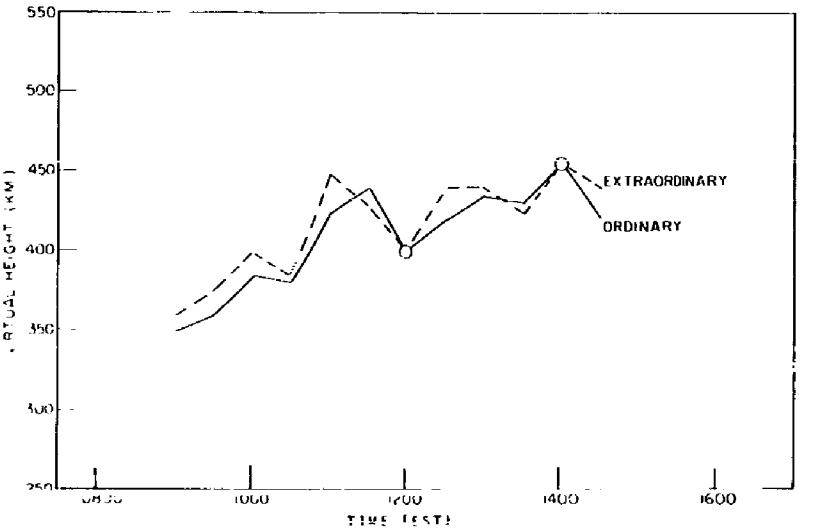

Fig. 46 - Virtual height vs time, Ft. Belvoir ionogram for Dec. 23, 1957, transponder at Clarendon, Texas

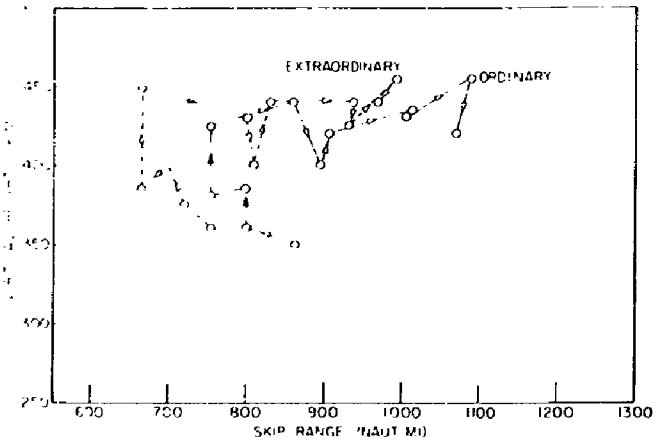

Fig. 47 - Virtual height vs skip range, Ft. Belvoir ionogram for Dec. 23, 1957, transponder at Clarendon, Texas

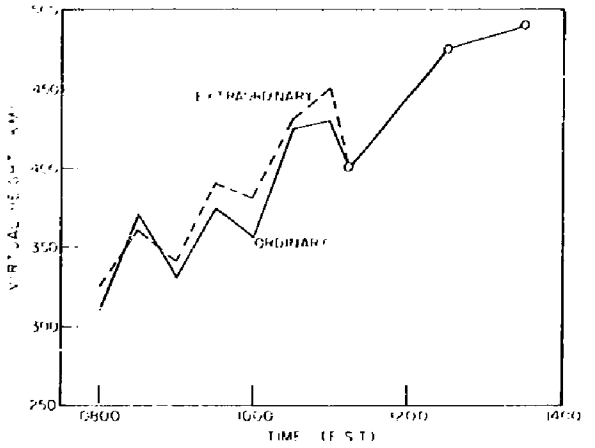

Fig. 48 - Virtual height vs time, White Sands ionogram for Dec. 23, 1957, transponder at Clarendon, Texas

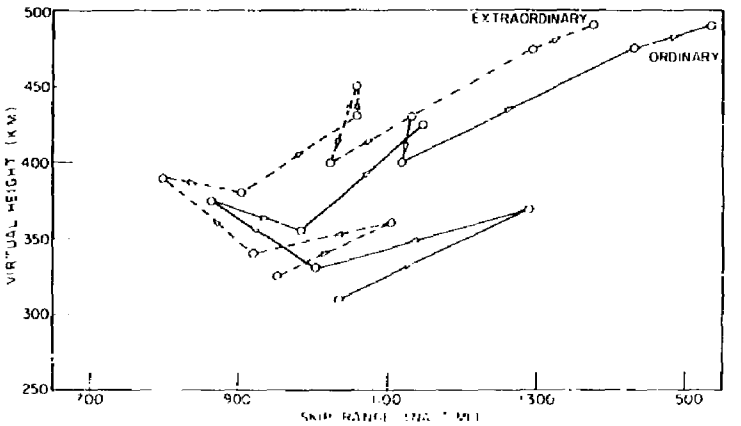

Fig. 49 - Virtual height vs skip range, White Sands ionogram for Dec. 23, 1957, transponder at Clarendon, Texas

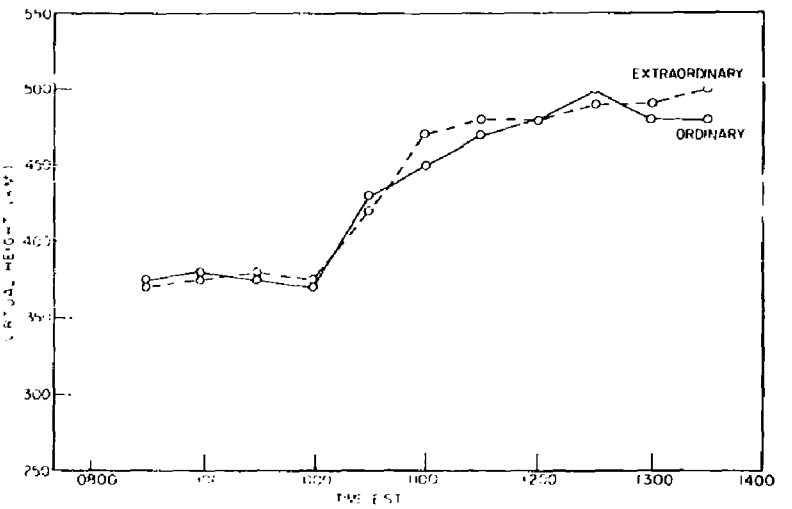

Fig. 50 - Virtual height vs time, Ft. Belvoir ionogram for Dec. 26, 1957, transponder at Clarendon, Texas

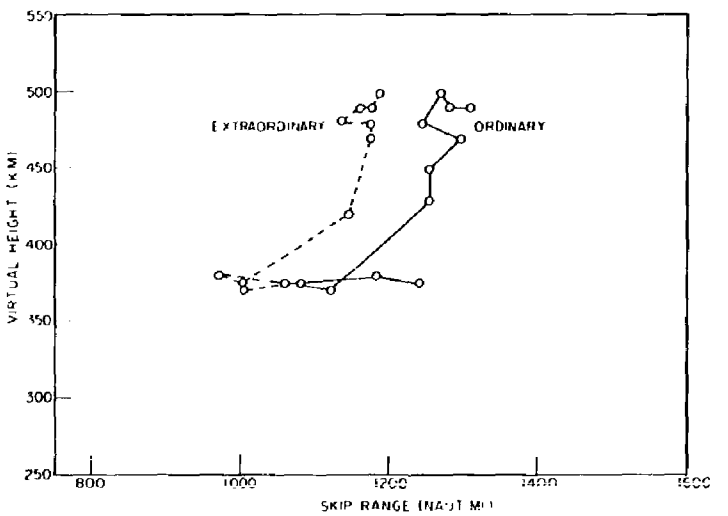

Fig. 51 - Virtual height vs skip range, Ft. Belvoir ionogram for Dec. 26, 1957, transponder at Clarendon, Texas

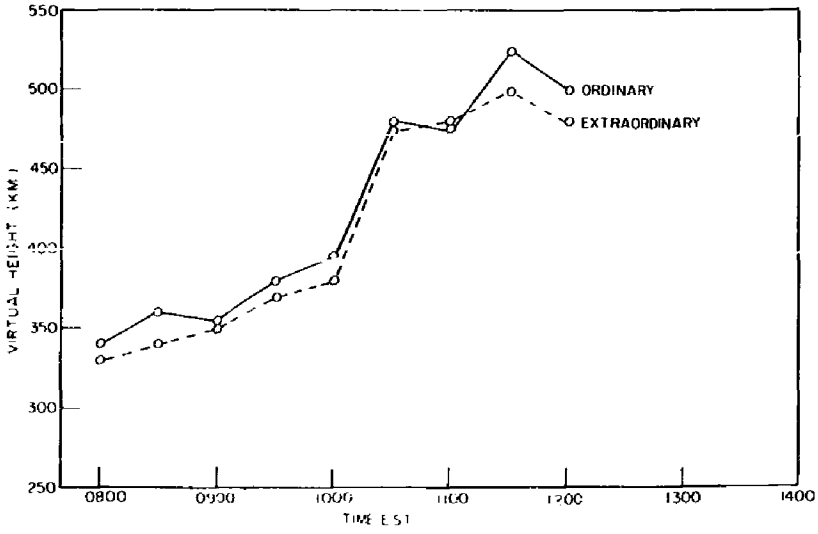

Fig. 52 - Virtual height vs time, White Sands ionogram for Dec. 26, 1957, transponder at Clarendon, Texas

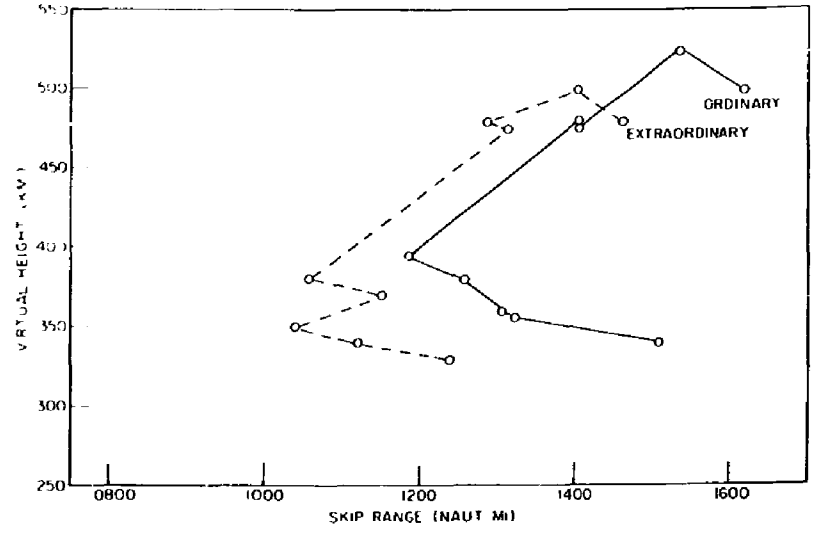

Fig. 53 - Virtual height vs skip range, White Sands ionogram for Dec. 26, 1957, transponder at Clarendon, Texas

* * *

CONFIDENTIAL

CONFIDENTIAL

UNITED STATES GOVERNMENT

memorandum

5300-31
DATE: 29 June 1998

REPLY TO ATTN OF: Code 5300

SUBJECT: REQUEST TO DECLASSIFY NRL REPORTS

TO: Code 1221.1 (C. Rogers)

1. It is requested that the NRL Reports listed below be declassified. The information contained in these reports has become public knowledge in the many years since first classified.

Declassified, public release.

3706 AD-C954460	4371 AD-038472 ✓	[redacted]	[redacted]	5338 AD-312117 ✓	[redacted]
[redacted]	[redacted]	[redacted]	[redacted]	5399 AD-314113 ✓	5540 AD-320263 ✓
[redacted]	[redacted]	5126 AD162728 ✓	5247 AD-304547 ✓	5403 AD-312699 ✓	5570 AD-320953 ✓
[redacted]	[redacted]	[redacted]	[redacted]	5441 AD-315354 ✓	
4284 AD031076 ✓	4878 AD-125352 ✓	5197 AD302457 ✓	[redacted]	5536 AD-343165 ✓	

Declassify, DoD and DoD contractors only.

4500	5511
5000A	5564
5508	

Will Send Later
TKS
Mary Templeman

G. V. Trunk

G.V. TRUNK
Superintendent
Radar Division